Hindawi
Geofluids
Volume 2017, Article ID 4818207, 12 pages
https://doi.org/10.1155/2017/4818207

Research Article

Remarkable Preservation of Microfossils and Biofilms in Mesoproterozoic Silicified Bitumen Concretions from Northern China

Xiaomei Wang,[1] Shuichang Zhang,[1] Huajian Wang,[1] Donald E. Canfield,[2] Jin Su,[1] Emma U. Hammarlund,[2] and Lizeng Bian[3]

[1]*Key Laboratory of Petroleum Geochemistry, Research Institute of Petroleum Exploration and Development, China National Petroleum Corporation, Beijing 100083, China*
[2]*Institute of Biology and Nordic Center for Earth Evolution (NordCEE), University of Southern Denmark, Campusvej 55, 5230 Odense M, Denmark*
[3]*Department of Geosciences, Nanjing University, Nanjing 210093, China*

Correspondence should be addressed to Shuichang Zhang; sczhang@petrochina.com.cn

Received 31 March 2017; Accepted 21 August 2017; Published 27 September 2017

Academic Editor: John A. Mavrogenes

Prokaryotes, often generally referred to as "bacteria," are the original and thus oldest life on Earth. They have shaped the chemical environment of the Earth, but they are difficult to find as ancient fossils due to their subtle structure. Here we report well-preserved fossilized microbial communities in silicified bitumen concretions from unit 3 of the Xiamaling Formation (1.39 Ga) in northern China. The numerous silicified bitumen concretions are in a variety of forms including ellipsoidal, spindle, and pancake ones, with diameters of 1~16 cm and thicknesses of 0.5~3 cm. The principal planes of the concretions are at low angle or directly parallel to the depositional plane level, showing obvious depositional characteristics. The concretions are silicified with abundant bitumen inside. Many different kinds of microbial fossils are found in the bitumen, including spherical forms, rods, and filaments, and some of the microbes are aggregated together in the forms of multicellular structures. These concretions preserve a delicate Mesoproterozoic biotic community.

1. Introduction

The Mesoproterozoic Era (1.6–1.0 Ga) is intermediate between the generally well-oxygenated Earth-surface conditions of the Phanerozoic Eon and the generally anoxic Archean Eon. The Mesoproterozoic Era was also a time evolutionary transition with the emergence of eukaryotic communities [1–4], although some argue that it is an Era of geochemical stagnation, the so-called "boring billion" [5, 6]. To better understand the nature and evolution of the ancient biosphere, including the ecology of paleoenvironments, we can potentially probe the ancient fossil records. There are some reports of Mesoproterozoic fossils about the discovery of eukaryotes all over the world [7–10], including the acritarchs with circular excystment, multilayered walls, or ornamentation, multicellular filaments, and algal thallus [11], string-of-beads fossils named *Horodyskia moniliformis* and *Horodyskia williamsii* from shales in the 1.48 Ga lower Appekunny Argillite of Glacier National Park [12], diverse eukaryotic fossils like *Tappania plana* from the Early Mesoproterozoic Roper Group in Australia, and *Horodyskia moniliformis* from the Mesoproterozoic Bangemall Group [13]. Even the possible crown-group multicellular rhodophytes in 1.6 Ga Lower Vindhyan Supergroup in central India were reported, antedating the oldest previously accepted red alga in the fossil record by about 400 million years [14].

While it is generally shown that Mesoproterozoic microfossils are characterized by cyanobacteria, unfortunately, insights into the behavior of ancient bacteria, especially during the Proterozoic Eon, are hampered by a sparse geological record [15, 16]. Thus, unlike the later emerging and fossilizable animal hard parts [17], microbes in general,

and prokaryotes in particular, have tiny body size and weak structures that are very difficult to fossilize and preserve [18]. Therefore, there are relatively few reports of bacteria fossils in their natural settings, although the compressed, straight, circular to sinuously coiled megascopic and helical carbonaceous fossils including *Grypania spiralis* and *Katnia singhi* in the Early Mesoproterozoic Rohtas Formation in India were believed to be possible cyanobacterial origin [19].

We note, however, that early silicification offers a potential avenue for microbial fossilization, preserving some of the oldest fossils known in the geologic record. Thus, some of the earliest microfossils are in shallow-marine silicified deposits (3.2 Ga) [20], or they adhere to the detrital quartz grains of their host sediments (3.4 Ga) [21]. Here we report some well-preserved bacterial communities from the unit 3 of Xiamaling Formation, northern China, in Mesoproterozoic Era. The fossilized organisms, observed in what appear to be different forms, provide direct evidence of ancient bacterial biomass records in Mesoproterozoic Era.

2. Geological Setting

The Xiamaling Formation is deposited on the North China Platform and immediately overlying the Tieling dolomite. The age of the Xiamaling Formation has been constrained to 1392.2 ± 1.0 Ma for the bentonite layer at the top of unit 3 and 1384.4 ± 1.4 Ma for the tuff layer 52 m above the bentonite [22]. Sediments of the Xiamaling Formation began their deposition at ~1,400 Ma at paleolatitude between 10°N and 30°N (with an uncertainty of some 10° latitude) [23].

We previously divided the Xiamaling Formation informally into 6 units [24]. Units 5 and 6 have yet to fully described, whereas unit 4 comprises alternating iron oxide-rich and iron oxide-poor sediments or repeating bundles of alternating sediment type, grading upwards into alternating layers of black shale and chert of unit 3 and further upwards into unit 2 comprised predominantly of black shale alternating with grey and black silty mudstones [22, 24]. Uppermost unit 1 is composed of alternating layers of black and green shales. Black shales are very common in all of the Xiamaling Formation, except for the lowermost 2 units. The total organic carbon (TOC) of the Xiamaling Formation ranges from less than 1 wt% in the green and red sandy mudstones to over 10 wt% in the black shales [22]. Our previous work suggests that the sediment geochemical fluctuations reflect the orbital forced changes, known as Milankovitch cycles, controlled the wind patterns, rainfall, and ocean circulation, and then translated into sediment geochemistry [22].

In addition to the highly fluctuating sedimentation, we also found concretions and bitumen in unit 3 of the Xiamaling Formation (Figure 1). Most of the concretions occurred at low angle or parallel to the depositional plane, embedded in the surrounding black shales or green chert (Figures 1(b) and 1(c)). The concretions were ellipsoidal or pie-like in form, with diameters in the range of 1 to 16 cm and thicknesses in the range of 0.5 to 5 cm (Figures 1(d) and 1(e)). Spherical or granular soft materials could be seen with black gloss and a smell of bitumen after the ellipsoidal concretions were broken. After a few minutes of exposure, visible color variation could be observed on the fresh surface of the internal bitumen, due to the possible oxidization of reactive iron. These observations suggest that the concretions are well closed within an internal reducing environment. Nonconcretionary bitumen layers or small round bitumen granules were also found sandwiched in the black and green shales, but no bacterial fossils were found in these bitumen types (Figures 1(f) and 1(g)).

3. Materials and Methods

Well-preserved bitumen concretions were carefully separated from the surrounding rocks and were then progressively cleaned with diluted hydrochloric acid (10%), distilled water, and high purity chloroform to remove exterior contaminations. Whole concretions, external shell, and internal bitumen were imaged in three dimensions (3D) through X-ray layer mapping.

Because of the fragility of the bitumen, it was impossible to cut through them with a saw. Instead, the bitumen was opened by breaking. Small bitumen samples were ground to powders and analyzed for elemental and biomarker composition. For comparison, the fresh surrounding rocks, including the black shales and green cherts, were also sampled, crushed, and analyzed. We attempted to make petrological thin sections to detect the structure of bitumen and the relationship of fossils and bitumen but failed due to the high fragility of the bitumen. Instead, we use scanning electron microscope (SEM; VEGA 3, TESCAN) to observe the bitumen for internal biological structures.

3.1. Morphological Imaging. 3D morphological imaging was performed by X-ray tomographic microscopy (XTM; XM-Tracer-225, Institute of High Energy Physics, China) at the Institute of High Energy Physics (IHEP), Chinese Academy of Sciences (CAS), China. A set of grey-level images were obtained. Then, the 3D structures of the concretions and their internal bitumen were rendered with high resolution (<27 μm) through image denoising, image enhancement, contour extraction, and triangular surface reconstruction with Amira® software.

Microscopic observations of the external shell and internal bitumen using scanning electron microscope were performed at the Key Laboratory of Petroleum Geochemistry (KLPG), China National Petroleum Corporation (CNPC). Fresh surfaces were gold-coated and photographed with the enlargement factor not lower than 10,000. Semiquantitative data of the major elements (C, O, Ca, Al, Fe, Mg, and Si) were gained with a coupled energy dispersive spectrometer [EDS].

3.2. Major Elements and Rare Earth Elements. The contents of major elements (Al, Ca, Si, and Fe) and rare earth elements (REEs) for the concretions and rock samples were obtained by X-ray fluorescence spectrometry (XRF; PW2404, Philips Electronics) and high-resolution inductively coupled plasma mass spectrometry (ICP-MS; Element I, Finnigan MAT) at the Key Laboratory of Petroleum Geochemistry (KLPG) at the China National Petroleum Corporation. Detailed analytical procedures can be found in Zhang et al. [26].

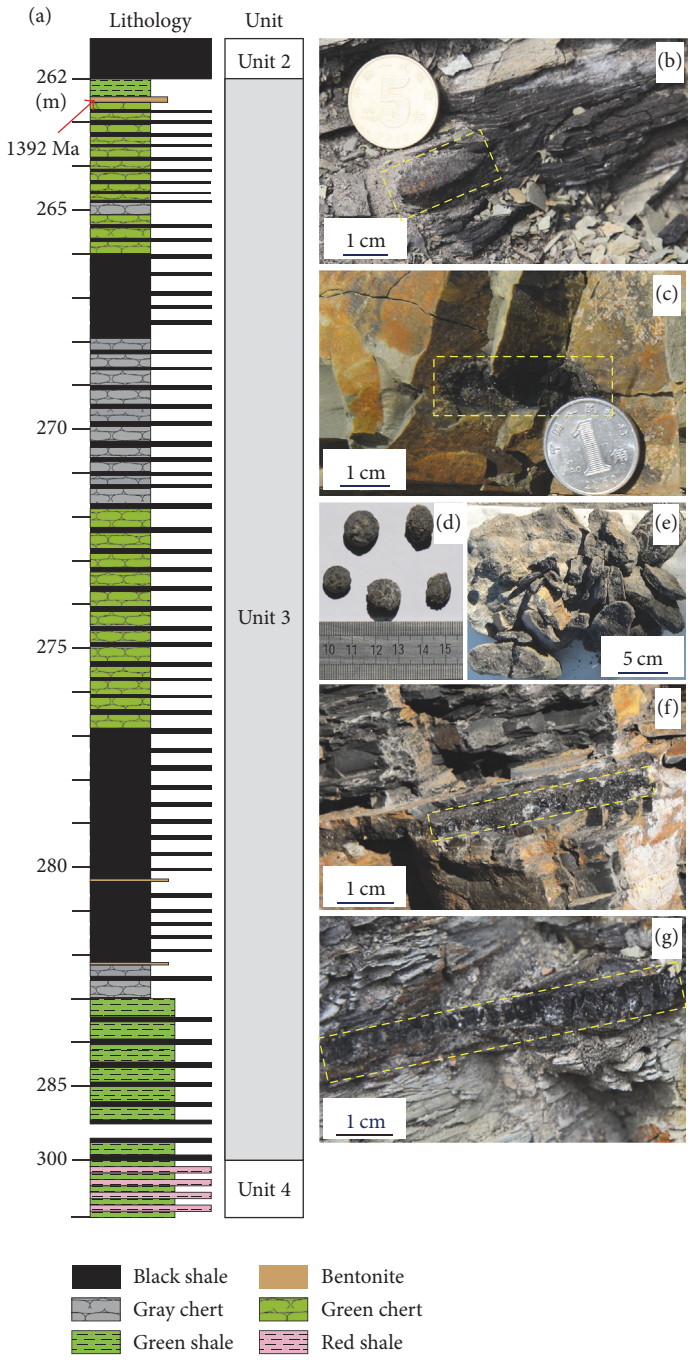

Figure 1: Generalized stratigraphy of unit 3 of Xiamaling Formation (a), representative photographs of the bitumen concretions embedded in black shales (b) and green cherts (c), the ellipsoidal or pie-like concretions (d-e), and the bitumen layers sandwiched between the black shales (f) and green shales (g).

Shale standard material (GBW 03014) was used to evaluate analytical accuracies, with the relative standard deviations (SD) of less than 1.0% for the major elements and less than 1.5% for the REEs.

4. Results

4.1. The Components of Concretions and Surrounding Rocks. XTM studies reveal an egg-like morphology for the concretions, with internal spherical cores and external dense shells (Figure 2). Rapid X-ray signal intensity changes between the shell and core imply large material density differences between the internal materials and external shell (Figure 3). XRF data show that the major component of the shell was silica (>90 wt%), at higher concentration than in the surrounding rocks (<60 wt% in the black shales and <90 wt% in the green chert) (Table 1). Correspondingly, the iron and aluminum contents in the concretion shells were

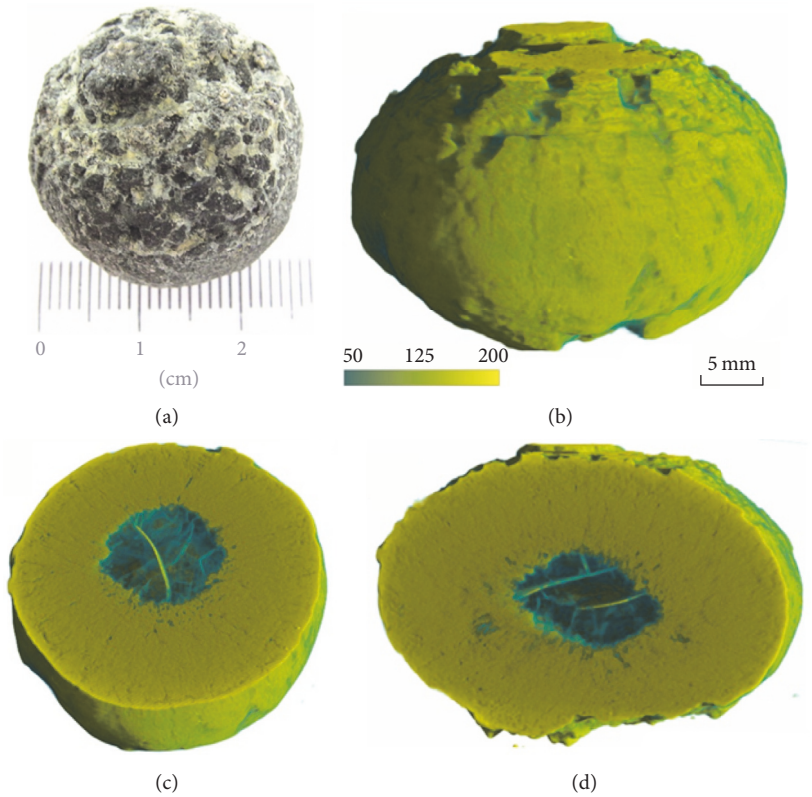

Figure 2: Selected ellipsoidal-type concretion (a) and the reconstructed three-dimensional imaging with resolution of 27 μm (b–d).

Table 1: Major and rare earth elements contents in the concretion shells and surrounding rocks.

Elements	Concretions in black shale		Surrounding black shale	Concretions in green chert		Surrounding green chert
	SC-BS-1	SC-BS-2		SC-GC-1	SC-GC-2	
SiO_2 (wt%)	90.10	89.03	58.53	90.70	93.26	85.90
Fe (wt%)	0.19	0.46	2.16	0.20	0.23	1.02
Ca (wt%)	0.45	0.47	0.85	0.77	0.90	0.29
Al (wt%)	0.04	0.07	4.58	0.04	0.06	3.06
La (μg/g)	0.34	0.52	30.60	0.69	0.53	13.10
Ce (μg/g)	1.14	0.52	56.80	0.29	0.08	25.80
Pr (μg/g)	0.17	0.21	7.28	0.17	0.17	3.31
Nd (μg/g)	0.93	1.11	30.80	0.59	0.65	12.80
Sm (μg/g)	0.64	0.08	5.62	0.03	0.13	2.72
Eu (μg/g)	0.13	0.12	0.85	0.05	0.04	0.47
Gd (μg/g)	0.23	0.23	4.84	0.10	0.13	2.29
Tb (μg/g)	0.03	0.18	0.88	0.07	0.10	0.40
Dy (μg/g)	0.20	0.18	5.84	0.15	0.13	2.5
Ho (μg/g)	0.03	0.04	1.14	0.03	0.03	0.52
Er (μg/g)	0.58	0.03	3.44	0.01	0.09	1.65
Tm (μg/g)	0.01	0.01	0.63	0.01	0.02	0.26
Yb (μg/g)	0.08	0.08	3.78	0.09	0.11	1.88
Lu (μg/g)	0.02	0.00	0.45	0.02	0.02	0.32
ΣREE (μg/g)	4.53	3.31	152.95	2.30	2.23	68.02
LREE (μg/g)	3.35	2.56	131.95	1.82	1.6	58.2
HREE (μg/g)	1.18	0.75	21	0.48	0.63	9.82
LREE/HREE	2.84	3.41	6.28	3.79	2.54	5.93

LREE: light rare earth elements, containing La, Ce, Pr, Nd, Sm, and Eu; HREE: heavy rare earth elements, containing Gd, Tb, Dy, Ho, Er, Tm, Yb, and Lu.

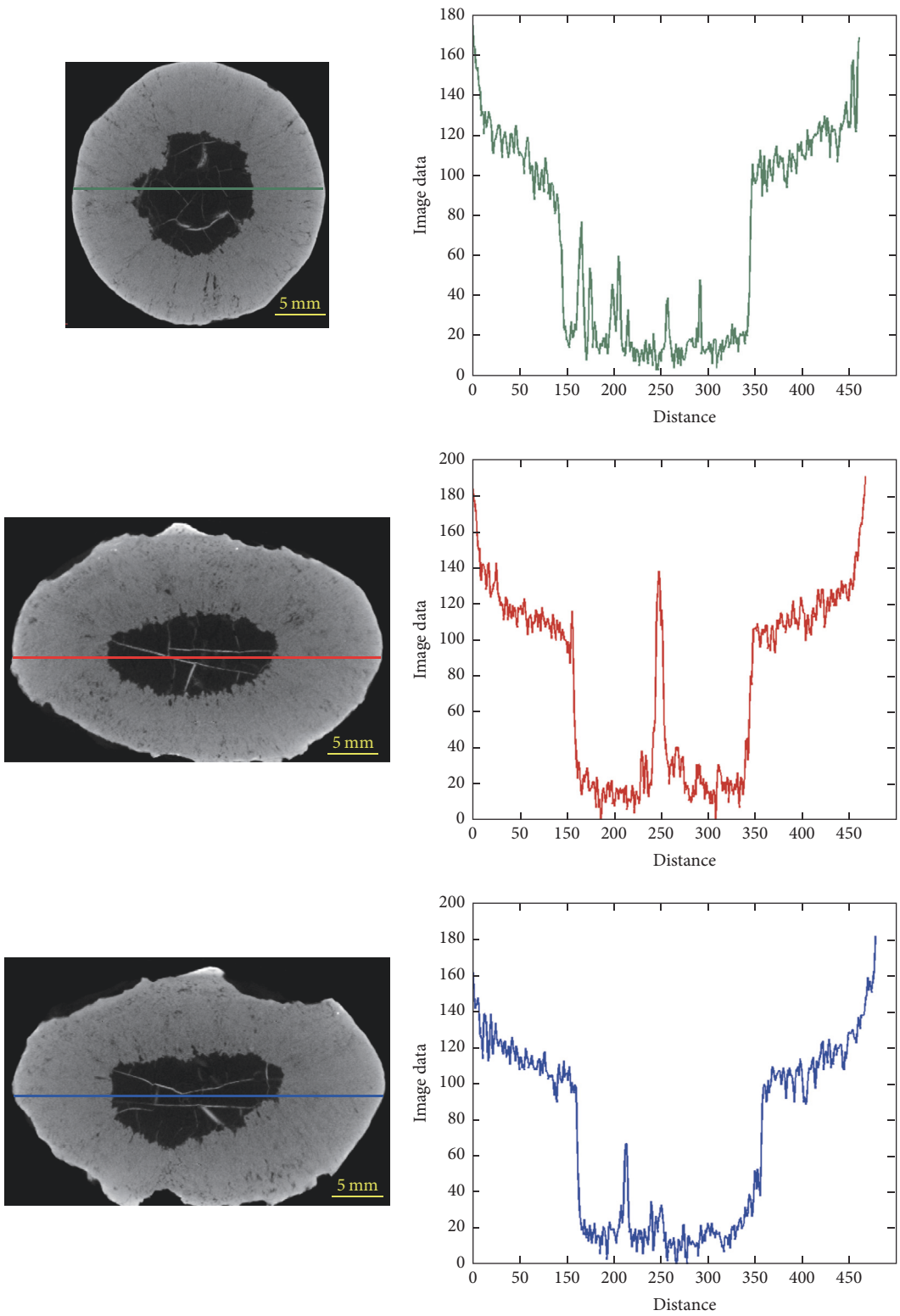

Figure 3: Sudden X-ray signal changes in the shell and core show great material density differences between internal and external substances. The concretion sample was the same as that in Figure 2.

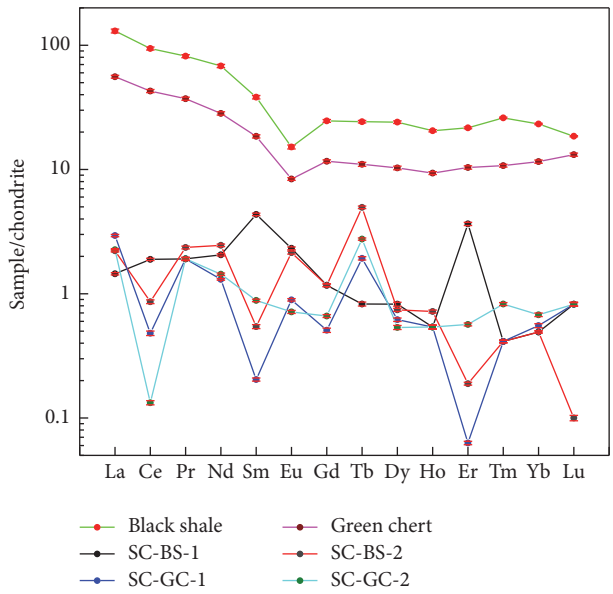

FIGURE 4: Chondrite-normalized REE patterns of the concretions and surrounding rocks in the Xiamaling Formation. SC-BS and SC-GC mean the silicified concretions in the black shales and green cherts, respectively. The contents of REEs of chondrite were referenced from [25].

much lower than those in the surrounding black shales or green cherts (Table 1).

The surrounding rocks had relatively high contents of ΣREE (~68.02 μg/g for cherts and ~152.95 μg/g for black shales), high light LREE element enrichment (~131.95 μg/g for black shales and 58.2 μg/g for cherts), and negative Eu anomalies ($Eu/Eu^* < 1$) for the chondritic normalized REE patterns. However, in contrast, the concretions had low contents of ΣREE (<5 μg/g) and light LREE elements enrichment (1.6~3.35 μg/g), a negative Ce anomaly, and a positive Eu anomaly ($Eu/Eu^* > 1$) (Figure 4 and Table 1).

EDS data showed high contents of carbon (~80 wt%) in the core, proving its organic origin. These internal core materials were soluble in chloroform, with a proportions of asphaltenes (~90 wt%), as is typical of bitumen (Table 2).

4.2. The Bacterial Fossils in the Concretions. Some of fossil-like biological structures were found scattering or embedding in the bitumen. Most of them had a smooth surface, but some were winkled, with a size range of 0.5~5 μm, a characteristic of prokaryotes [27, 28]. Energy Dispersive Spectra (EDS) analysis shows that the carbon content of biological structures could be up to >30%, much higher than the carbon content in regular carbonate minerals, suggesting these fossil-like substances might be bacterial fossils rather than mineral crystals [29, 30]. The contents of Si and O were 15%~27% and 0.5%~4%, respectively, indicating silicification of these possible microbial fossils. Of course there is possibility that Si and C could be from the bitumen substrates, so the EDS results for the biological structure just work as a reference value.

General parameters used to identify microbial fossils include their size, shape, and the chemical composition [29]. And comparison of modern and Precambrian living forms confirms the inference that cyanobacterial communities are very conservative and have changed insignificantly both morphologically and physiologically during the past two billion years [31]. So modern prokaryotes growing with a wide range of recognizable morphologies provide a general reference for fossil identification. We classify the fossil-like and biofilm-like structures scattered on or embedded in the surface of the bitumen into three major categories: spheres, rods, and vibrios, based on their shapes from SEM. Each of these is present with unique colonial organization.

4.2.1. Category 1: Sphere Shaped Structures. Most spheres are deflated, with a smooth and regular surface. The average diameter is about 1 μm. They scatter on the surface of the bitumen and surrounding silicolites. They are found dispersed, in couples, or clustered together (Figure 5). All of these shapes are similar to modern coccus bacteria, where modern cocci sometimes maintain a distinct arrangement after they divide, giving an important reference role in classification. Figures 5(a) and 5(b) are like modern monococcus, split on two dimensions. In Figures 5(c) and 5(d), every four cells formed together, like modern tetracoccus or staphylococcus. Figure 5(e) shows clusters of various size. Overall, whether found singly, in small groups or in biofilms, these forms show great similarity to modern coccoid bacteria. These fossils also display evidence for cell shrinkage and cell wall collapse into a vacated cytoplasmic space during fossilization (Figure 5). The spherical fossils also display regular stripes on the cell surface (Figures 5(b), 5(c), and 5(e)). Some fossils were also found closely packed in a possible extracellular polysaccharide matrix (EPS) (Figures 5(e) and 5(f)). The specific morphology of these structures, combined with their high carbon content, strongly suggest a biogenic origin (Figure 5).

We also find that many of these preserved structures coexisted in a small closed concretion. The subpolygonal honeycomb coccoid structures in the Xiamaling Formation show some wall-to-wall contact, with four or even more coccoids as neighbors (Figures 5(c)–5(e)). Also, some of the fossil forms, as shown in Figures 5(e) and 5(f), are reminiscent of microbial mats or biofilms. Nearly all of the observed forms including spherical, rod, and vibrioid forms display aggregated modes including sheets, chains, and biofilms.

4.2.2. Category 2: Rod-shaped Structures. Most of the rod-shaped forms are found in rods and cylinders, with blunt or sharp ends (Figure 6). The length and width are about 1.0 to 2.0 μm and 0.2 to 0.5 μm, respectively. These structures are presented singularly and in chains, with possible dissepiment structures within the fossil cells (Figures 6(j) and 6(k), as the arrow shows). These forms show a great deal of similarity with modern bacillus. Possible septum-like features may be the junction points for individual rod cells. For convenience of description, the rod structures are grouped into three categories.

Table 2: The group components of the internal materials in the concretions. The sample numbers were same as those in Table 1 and Figure 4.

	Saturates (wt%)	Aromatics (wt%)	Resins (wt%)	Asphaltenes (wt%)
SC-BS-1	2.56	5.48	2.21	89.75
SC-BS-2	1.24	5.73	3.60	88.43
SC-GC-1	2.21	4.71	2.85	90.23
SC-GC-2	1.85	6.48	3.72	87.95

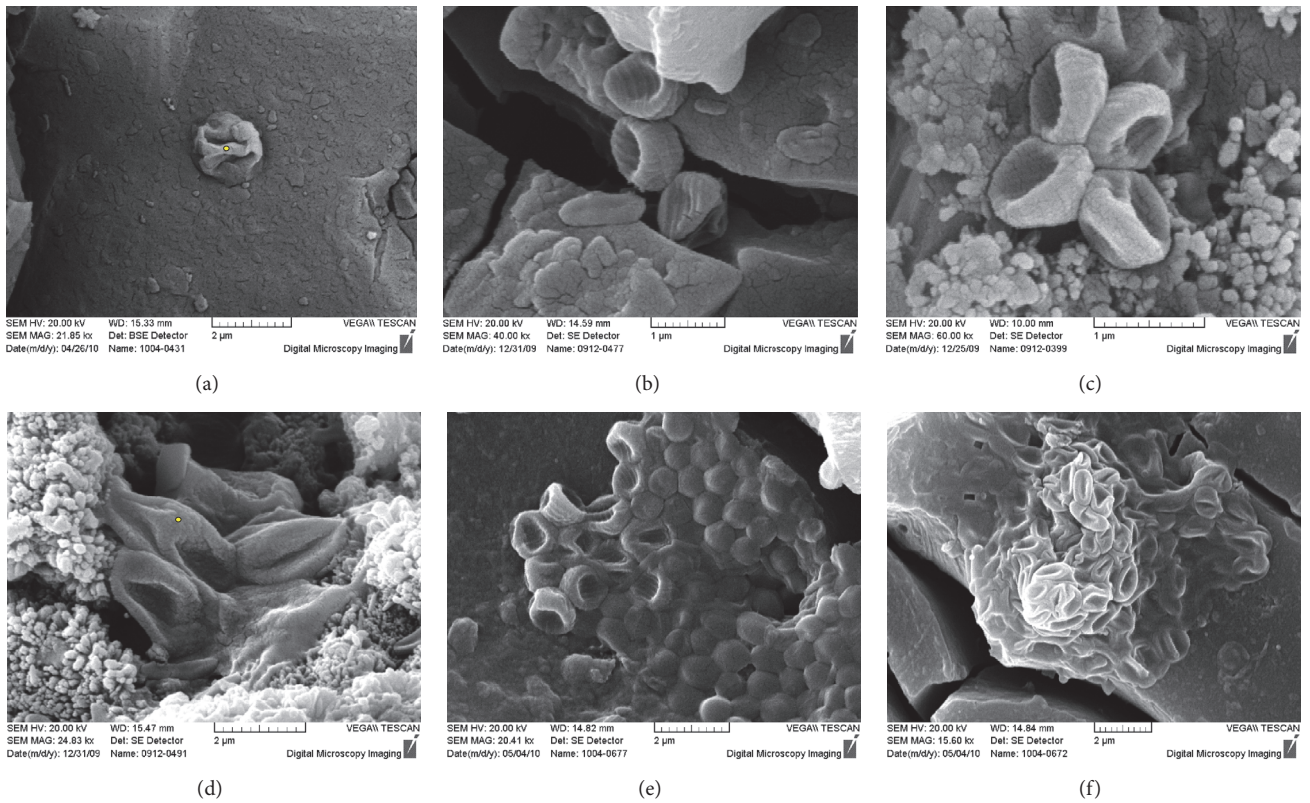

Figure 5: SEM photomicrographs of the spherical bacteria fossils and the colonial structures. EDS data of (a) and (d) were showed in Table 1.

Category 2a: Straight Rod and Round End (Figures 6(a)–6(c)). Single or several structures cluster together, projecting from the bitumen surface. They have straight and rounded ends, 1.5 to 5 μmin length and ca. 0.5 μm width. Rods are parallel-sided, with a smooth, clean appearance. The chemical composition is dominated by C, O, and Si. It is possible that the rod-shaped structures were originally bacteria that acted as a template for mineral deposition, which then replaced the organic material [32].

Category 2b: Curved Rod and Round End (Figures 6(g) and 6(h)). These structures are scattered on the surface of the bitumen and silicolites, with a curved structure and round end, 2 to 4 μm in length, 0.5 μm in width, presenting a smooth, clean appearance. They have the chemical composition of C, O, Si, and Fe or C, O, Si, and Ca.

Category 2c: Curved Rod and Sharp End (Figures 6(i)–6(m)). These structures have a good three-dimensional form. They occur in pairs or scattered on the surface of the bitumen and silicolites, with dissepiment sometimes in the middle of the structures, some evidence of cell division (Figure 6(m), as the arrow shows). These structures are usually slightly crooked with a length of ca. 2 μm, a width of 0.5 μm, and a smooth, clean appearance and sharp end. The chemical composition is mainly C, O, Fe, and Si.

These rod-shaped structures resemble the modern bacillus bacteria in their size range and distribution. Surfaces are usually smooth, occasionally granular. Some of the cells existed in chains of two or three through end-to-end contact, with possible internal channel in each cell (Figures 6(j), 6(k), and 6(m)).

4.2.3. Category 3: Navicula Structure (Figures 6(n) and 6(o)). This unusual feature is comprised of collapsed surfaces, traversed by deep grooves in the center of the structure. The structure has an overall length of ca. 2 μm, a width of ca. 0.4 μm, and a depth of ca. 0.2 μm, with a smooth, clean appearance, while having no ridges. Analyses showed a narrow range of elements C, O, and Si. The elongated

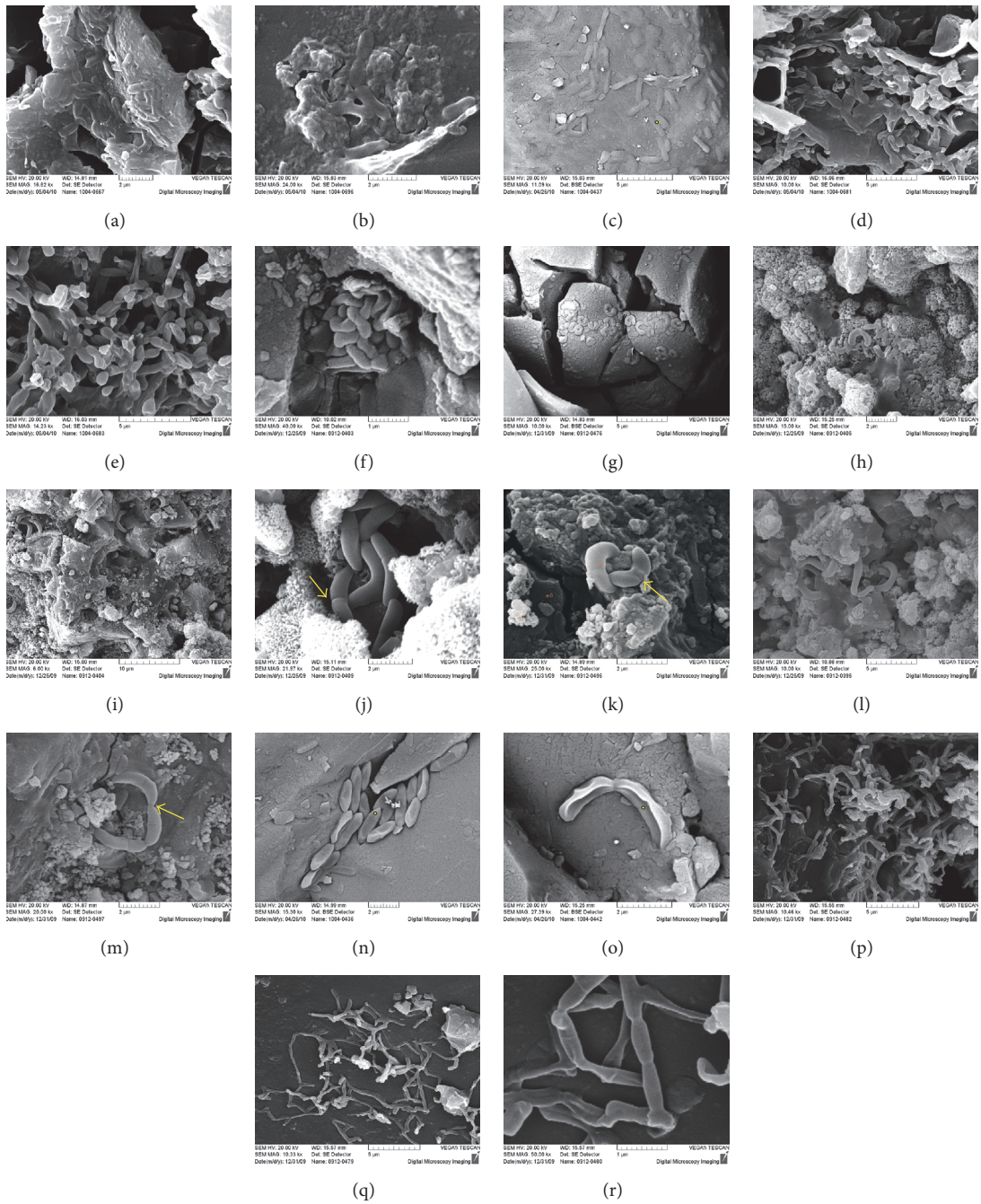

Figure 6: SEM photomicrographs of the rod bacteria fossils and biofilms. EDS data of (a), (b), and (c) were showed in Table 1.

grooves and wrinkles could be possibly presumably produced by dehydration.

4.2.4. Category 4: Filaments/Tubes Bacteria Fossils (Figures 6(p) and 6(r)). The surfaces of the individual units of the structure are irregularly undulating, very similar to the modern filamentous bacteria. The diameter of this possible filamentous fossil is 0.2 μm. The long units are divided into many cells by some structure like septate hyphae and the biomass could possibly assimilate nutriment by it. This kind of fossil structure shows C, Si, and traces of Al and Fe.

Anyway, some ancient bacteria-like forms have proven controversial [33–35], and some ancient fossil microbial forms are regarded as the result of the evaporation and precipitation of rocks or the transformation of soft sediment and the silicious solution [36, 37]. Thus, we appeal to general parameters used to establish microbial fossil biogenicity including the characteristics of size range, shape features, distribution abundance, and chemical compositions [29]. As prokaryotes have likely undergone little morphological evolution through Earth history, morphological comparison with modern bacteria provides the general reference guiding

our ancient bacterial fossil identification. Thus, in drawing conclusions as to whether these fossil microbes from the Xiamaling Formation are from the Mesoproterozoic Era, we appeal to the criteria used during similar interrogations of possible Precambrian prokaryote record [28, 38]. Based on above observations and discussion, we emphasize the observed structures are indigenously syngenetic microbes.

5. Discussions

5.1. The Age of Bacteria in the Concretions and the Microbial Affinity. The bitumen concretions found in both the black shales and green cherts of unit 3 of Xiamaling Formation have similar morphological structure and chemical compositions (Figures 1 and 4, Tables 1 and 2), suggesting similar formation pathways and timing, since the biomarkers of the bitumen and surrounding black shales are so similar, with almost the same hopanes and diahopanes series, such as C_{18}~C_{24} tricyclic terpanes, C_{24} tetracyclic terpane (C_{24TT}), 18α(H)-17α-methyl-22,29,30-trisnorhopane (Ts), 7α(H)-22,29,30-trisnorhopane (Tm), C_{29}~C_{34} hopanes, and the C_{19}~C_{22} long chain alkyl tricyclic terpanes ($^{*}C_{19}$~$^{*}C_{22}$), C_{29} preeluting [39], and the diahopanes of $^{*}C_{29}$, C_{29}Ts, and $^{*}C_{30}$, suggesting the bitumen should be originated locally from the black shales.

As the microbes are found within the bitumen inside the highly silicified concretions, they should occupy the bitumen before silicification or contemporaneous with the formation of concretion, not invaded later. Thus, the age of the microbes could be linked to the age of the concretions. Silicification could have resulted from either hydrothermal or digenetic processes, which can be distinguish based on REE patterns [40, 41]. Indeed, the concretions display exceptionally low contents of ΣREE, slight LREE enrichment, and occasional positive Eu anomalies, quite different from the patterns observed in the sedimentary chert (Figure 4). Therefore, the concretions did not form by simple digenetic remobilization of sedimentary chert, and the REE patterns themselves suggest another source for REE and possibly also for the silicon for the concretions [40]. Thus, the concretion formation might be related to a hydrothermal event.

Good candidates for hydrothermal activity are found in Zhaojiashan (about 10 kilometers away), Qinyu (about 100 kilometers away), and Kuancheng area (about 200 kilometers away), where, in each locality, 3~4 layers of intrusive diabase are found in the unit 3 of Xiamaling Formation. These have U-Pb isotope age of 1320 ± 6 Ma and 1327 ± 2.3 Ma [42, 43] and postdate deposition of unit 3 by about 70 million years. Therefore, the concretions housing bitumen-associated microbes might be silicified by a local heating of diabase intrusion at about 1320~1327 Ma, and before this, as the bitumen formed, microbes would have been attracted to the available organic matter provided by the bitumen. It is quite likely that the bitumen sustained the microbial population from the time of their colonization, some unknown time after sediment deposition at about 1390 Ma [22], continuing to the time when the bitumen silicified at about 1325 Ma.

The high contents of silicon in most of the microfossils (Table 1) demonstrate the critical role of silica-saturated water in promoting fossil preservation. Experiments of artificially silicified microorganisms have demonstrated that most microbial cells were generally silicified through the silicification of the outer cell membrane, which might have resulted in the bacterial apoptosis and left the silicified membrane intact [44]. Of course, most of time, the cells will likely lose their cytoplasm through the silicification process, and their original three-dimensional shapes also might change as seen in Figures 5 and 6. Anyway, the microbes themselves were preserved in silica during this silicification process, leading to their exquisite preservation.

5.2. The Ecological Meaning. These ancient microbes are intimately associated with Xiamaling Formation bitumen and therefore likely occupied the deep biosphere at sufficient depth or temperature for bitumen formation to occur, since the bitumen of unit 3 is ranked as either immature or of early thermal maturity, indicating that the heating temperatures should be about 90°C [45]. Combining the size, shape, surface features, dissepiment, and the biological association, we can get the conclusion that most of the fossils should not be crystals of the permineralizing agent or migrated through fissure and fracture, but mineralized bacterial cells. It is, unfortunately, impossible from morphological considerations alone to identify the exact physiology of any of these organisms. The microbes are not associated with pyrite so sulfate reduction seems an unlikely metabolism. In the lack of any other metabolic oxidants (iron and manganese oxides and nitrate, e.g.), it would seem likely that the microbes were involved in either fermentation or possibly also methanogenesis, but it is difficult to say much more than this.

The aggregated bacterial populations adhere to each other on the bitumen as found in typical biofilms [46, 47], where microbial cells are typically embedded in EPS [48]. Indeed, the cells in Figures 5(e) and 5(f) seem to be preserved in a fossilized extracellular EPS-like matrix. Anyway, all of these aggregated bacteria likely form a consortia life style, a major form of microbial life, although this life style is poorly discussed and often confused with species-specific defense mechanisms. The consortia life style benefit is a number of aspects of life and the economical utilization of critical resources [49], making microbial respond to their specific microenvironmental conditions [50]. Also this life style forms some secondary structures as an attempt to benefit a population such as aiding in the search for food, resisting aggression, or striving for better life style [51, 52]. These kinds of bacterial aggregations might indicate some cooperative, unselfish behavior of the individual members like multicellular organisms. Some bacteria might also maintain their primary metabolism and physical characteristics, while others may be more altruistic to small size, collapsed, or wrinkled (Figures 5, 6(n), and 6(o)). Previous researches have shown that the aggregated life styles as found in biofilms represent a stable juxtaposition of cells and physiological cooperation and are much more efficient for living than mixed populations of free-living planktonic organisms [53, 54]. Whether these fitness advantages benefited the survival of the whole original bacteria population still needs to be confirmed.

The aggregated bacterial colonies form partially overlapping, locally recruited microcommunities. The single cells might represent noncooperating individuals, a prologue of the collapsed microcommunity [55], while the aggregated bacteria in these bitumen concretions constitute a stable microbial ecosystem. We can speculate that the aggregated bacterial species communicated via secreted molecules or through cell-cell contacts in what may have been a demonstration of social behavior [56], an essential trait of organisms. In another possible expression of communication, some of the spherical fossils have regular stripes, similar to the distinctive striations of "cable" bacteria, where the striations contain conductive materials allowing the transport of electrons over long distances of a cm or more [57].

There are fundamental distinctions between bacteria and multicellular organisms, although there are indeed similarities between biofilm bacteria, aggregated colonies in our bitumen, and multicellular organisms exhibiting some cooperative, unselfish behaviors [58]. In any event, the discovery of fascinating biofilm fossils and their physical cell-to-cell contact within biofilms shows that prokaryotes might have been well adapted to their surroundings and communicated and coordinated for the benefit of the whole community, a type of microbial behavior that existed since the Mesoproterozoic Era.

6. Conclusions

Although Mesoproterozoic Era is widely disputed between biological evolutionary stagnation time and macroscopic multicellular eukaryotic diversified time, our research from body fossils and molecule fossils declares that the bacteria is still the dominated biomass at that time. The silicified concretions in Xiamaling Formation have exquisite three-dimensional bacteria colonies in a remarkable state of preservation. The bitumen acted as matrix for microbe life to provide food. The microbe should be indigenous bacteria according to the judging criterion. According to the biomarker comparison, the bitumen in the core of the concretion should come from the surrounding black shales, with the help of hydrothermal activity and later silicification with the bacteria by the thermal water. So the age of bacteria should be 1.32 Ga, likely contemporaneous with the age of the nearby intrusive diabase. Although some bacteria form in biofilms or aggregates, they are not multicellular organisms, just illustrating the early state of cooperative, unselfish behaviors, having great ecology meaning. Therefore, the bitumen concretions provide an ideal living space for the bacteria in Mesoproterozoic Eon.

Conflicts of Interest

The authors declare that there are no conflicts of interest regarding the publication of this paper.

Acknowledgments

The research is financially supported by National Science and Technology Major Project (2016ZX05004-001), Strategic Priority Research Program of the Chinese Academy of Sciences (XDA14010101), State Key Program of National Natural Science Foundation of China (41530317), the Scientific Research and Technological Development Project of China National Petroleum Corporation (CNPC 2016A-0204), Danish National Research Foundation (DNRF53), the ERC (Oxygen Grant no. 267233), the Villum Foundation, and the Danish Council for Independent Research. The authors thank Dr. Zhang Kai at the X-ray Imaging Beamline 4W1A of the Beijing Synchrotron Radiation Facility (BSRF) and Dr. Wang Yanfang of the Key Laboratory of Nuclear Analysis in the Institute of High Energy Physics for their great help in the X-ray tomographic microscopy (XTM) studies and the tomographic reconstruction.

References

[1] N. J. Butterfield, "*Bangiomorpha pubescens* n. gen., n. sp.: implications for the evolution of sex, multicellularity, and the Mesoproterozoic/Neoproterozoic radiation of eukaryotes," *Paleobiology*, vol. 26, no. 3, pp. 386–404, 2000.

[2] E. J. Javaux, "Palaeontology: Microfossils from early Earth," *Nature Geoscience*, vol. 4, no. 10, pp. 663-664, 2011.

[3] A. H. Knoll, "The early evolution of eukaryotes: A geological perspective," *Science*, vol. 256, no. 5057, pp. 622–627, 1992.

[4] A. H. Knoll and E. A. Sperling, "Oxygen and animals in Earth history," *Proceedings of the National Academy of Sciences of the United States of America*, vol. 111, no. 11, pp. 3907-3908, 2014.

[5] M. D. Brasier and J. F. Lindsay, "A billion years of environmental stability and the emergence of eukaryotes: new data from northern Australia," *Geology*, vol. 26, no. 6, pp. 555–558, 1998.

[6] R. Buick, D. J. Des Marais, and A. H. Knoll, "Stable isotopic compositions of carbonates from the Mesoproterozoic Bangemall group, northwestern Australia," *Chemical Geology*, vol. 123, no. 1-4, pp. 153–171, 1995.

[7] Y. Leiming, Y. Xunlai, M. Fanwei, and H. Jie, "Protists of the upper mesoproterozoic Ruyang Group in Shanxi Province, China," *Precambrian Research*, vol. 141, no. 1-2, pp. 49–66, 2005.

[8] B. Rasmussen, I. R. Fletcher, J. J. Brocks, and M. R. Kilburn, "Reassessing the first appearance of eukaryotes and cyanobacteria," *Nature*, vol. 455, no. 7216, pp. 1101–1104, 2008.

[9] M. Sharma and Y. Shukla, "Taxonomy and affinity of early mesoproterozoic megascopic helically coiled and related fossils from the rohtas formation, the vindhyan supergroup, India," *Precambrian Research*, vol. 173, no. 1-4, pp. 105–122, 2009a.

[10] S. Zhu, M. Zhu, A. H. Knoll et al., "Decimetre-scale multicellular eukaryotes from the 1.56-billion-year-old gaoyuzhuang formation in north China," *Nature Communications*, vol. 7, Article ID 11500, 2016.

[11] Y. Leiming and Y. Xunlai, "Radiation of Meso-Neoproterozoic and Early Cambrian protists inferred from the microfossil record of China," *Palaeogeography, Palaeoclimatology, Palaeoecology*, vol. 254, no. 1-2, pp. 350–361, 2007.

[12] G. J. Retallack, K. L. Dunn, and J. Saxby, "Problematic Mesoproterozoic fossil Horodyskia from Glacier National Park, Montana, USA," *Precambrian Research*, vol. 226, pp. 125–142, 2013.

[13] A. H. Knoll, E. J. Javaux, D. Hewitt, and P. Cohen, "Eukaryotic organisms in Proterozoic oceans," *Philosophical Transactions of the Royal Society B: Biological Sciences*, vol. 361, no. 1470, pp. 1023–1038, 2006.

[14] S. Bengtson, T. Sallstedt, V. Belivanova, and M. Whitehouse, "Three-dimensional preservation of cellular and subcellular structures suggests 1.6 billion-year-old crown-group red algae," *PLoS Biology*, vol. 15, no. 3, Article ID e2000735, 2017.

[15] S. P. Diggle, A. S. Griffin, G. S. Campbell, and S. A. West, "Cooperation and conflict in quorum-sensing bacterial populations," *Nature*, vol. 450, no. 7168, pp. 411–414, 2007.

[16] G. M. Dunny, T. J. Brickman, and M. Dworkin, "Multicellular behavior in bacteria: Communication, cooperation, competition and cheating," *BioEssays*, vol. 30, no. 4, pp. 296–298, 2008.

[17] C. R. Marshall, "Explaining the Cambrian "explosion" of animals," *Annual Review of Earth and Planetary Sciences*, vol. 34, pp. 355–384, 2006.

[18] C. P. Marshall, J. R. Emry, and A. O. Marshall, "Haematite pseudomicrofossils present in the 3.5-billion-year-old Apex Chert," *Nature Geoscience*, vol. 4, no. 4, pp. 240–243, 2011.

[19] M. Sharma and Y. Shukla, "Taxonomy and affinity of early mesoproterozoic megascopic helically coiled and related fossils from the rohtas formation, the vindhyan supergroup, India," *Precambrian Research*, vol. 173, no. 1-4, pp. 105–122, 2009b.

[20] E. J. Javaux, C. P. Marshall, and A. Bekker, "Organic-walled microfossils in 3.2-billion-year-old shallow-marine siliciclastic deposits," *Nature*, vol. 463, no. 7283, pp. 934–938, 2010.

[21] D. Wacey, M. R. Kilburn, M. Saunders, J. Cliff, and M. D. Brasier, "Microfossils of sulphur-metabolizing cells in 3.4-billion-year-old rocks of Western Australia," *Nature Geoscience*, vol. 4, no. 10, pp. 698–702, 2011.

[22] S. Zhang, X. Wang, E. U. Hammarlund et al., "Orbital forcing of climate 1.4 billion years ago," *Proceedings of the National Academy of Sciences of the United States of America*, vol. 112, no. 12, pp. E1406–E1413, 2015.

[23] S. Zhang, Z.-X. Li, D. A. D. Evans, H. Wu, H. Li, and J. Dong, "Pre-Rodinia supercontinent Nuna shaping up: A global synthesis with new paleomagnetic results from North China," *Earth and Planetary Science Letters*, vol. 353-354, pp. 145–155, 2012.

[24] X. Wang, S. Zhang, H. Wang et al., "Oxygen, climate and the chemical evolution of a 1400 million year old tropical marine setting," *American Journal of Science*, vol. 317, 2017.

[25] R. F. Anderson, M. Q. Fleisher, and A. P. LeHuray, "Concentration, oxidation state, and particulate flux of uranium in the Black Sea," *Geochimica et Cosmochimica Acta*, vol. 53, no. 9, pp. 2215–2224, 1989.

[26] S. Zhang, X. Wang, H. Wang et al., "Sufficient oxygen for animal respiration 1,400 million years ago," *Proceedings of the National Academy of Sciences of the United States of America*, vol. 113, no. 7, pp. 1731–1736, 2016.

[27] J. W. Schopf and M. Walter, "Biofilms: microbial interactions and metabolic activities," in *Earth's Earliest Biosphere: Its origin and evolution*, pp. 21–51, Princeton University Press, Princeton, NJ, USA, 1983.

[28] F. Westall and R. L. Folk, "Exogenous carbonaceous microstructures in Early Archaean cherts and BIFs from the Isua Greenstone Belt: Implications for the search for life in ancient rocks," *Precambrian Research*, vol. 126, no. 3-4, pp. 313–330, 2003.

[29] F. Westall, M. J. De Wit, J. Dann, S. Van der Gaast, C. E. J. De Ronde, and D. Gerneke, "Early archean fossil bacteria and biofilms in hydrothermally-influenced sediments from the Barberton greenstone belt, South Africa," *Precambrian Research*, vol. 106, no. 1-2, pp. 93–116, 2001.

[30] J. W. Schopf, "Fossil evidence of Archaean life," *Philosophical Transactions of the Royal Society B: Biological Sciences*, vol. 361, no. 1470, pp. 869–885, 2006.

[31] L. V. N. Sergeev, M. Gerasimenko, and G. A. Zavarzin, "Comparison of modern and Precambrian living forms confirms the inference that cyanobacterial communities are very conservative and have changed insignificantly both morphologically and physiologically during the past two billion years," *Microbiology*, vol. 71, pp. 623–637, 2002.

[32] D. Edwards, L. Axe, J. Parkes, and D. Rickard, "Provenance and age of bacteria-like structures on mid-Palaeozoic plant fossils," *International Journal of Astrobiology*, vol. 5, no. 2, pp. 109–142, 2006.

[33] J. W. Schopf, A. B. Kudryavtsev, D. G. Agresti, T. J. Wdowiak, and A. D. Czaja, "Laser-Raman imagery of Earth's earliest fossils," *Nature*, vol. 416, no. 6876, pp. 73–76, 2002.

[34] M. D. Brasier, O. R. Green, A. P. Jephcoat et al., "Questioning the evidence for Earth's oldest fossils," *Nature*, vol. 416, no. 6876, pp. 76–81, 2002.

[35] M. D. Brasier, O. R. Green, J. F. Lindsay, N. McLoughlin, A. Steele, and C. Stoakes, "Critical testing of Earth's oldest putative fossil assemblage from the ~3.5 Ga Apex chert, Chinaman Creek, Western Australia," *Precambrian Research*, vol. 140, no. 1-2, pp. 55–102, 2005.

[36] F. G. Ferris, W. S. Fyfe, and T. J. Beveridge, "Metallic ion binding by Bacillus subtilis: Implications for the fossilization of microorganisms," *Geology*, vol. 16, no. 2, pp. 149–152, 1988.

[37] D. R. Lowe, "Abiological origin of described stromatolites older than 3.2 Ga," *Geology*, vol. 22, no. 5, pp. 387–390, 1994.

[38] J. Schopf and M. Walter, *a. Earths earliest biosphere: Its origin and evolution*, Princeton University, Princeton, 1983.

[39] J. M. Moldowan, F. J. Fago, R. M. K. Carlson et al., "Rearranged hopanes in sediments and petroleum," *Geochimica et Cosmochimica Acta*, vol. 55, no. 11, pp. 3333–3353, 1991.

[40] M. Bau, "Rare-earth element mobility during hydrothermal and metamorphic fluid-rock interaction and the significance of the oxidation state of europium," *Chemical Geology*, vol. 93, no. 3-4, pp. 219–230, 1991.

[41] A. W. Hofmann, "Chemical differentiation of the Earth: the relationship between mantle, continental crust, and oceanic crust," *Earth and Planetary Science Letters*, vol. 90, no. 3, pp. 297–314, 1988.

[42] H.-K. Li, S.-N. Lu, H.-M. Li et al., "Zircon and beddeleyite U-Pb precision dating of basic rock sills intruding Xiamaling Formation, North China," *Geological Bulletin of China*, vol. 28, no. 10, pp. 1396–1404, 2009.

[43] Y. Liu, N. Zhong, Y. Tian, W. Qi, and G. Mu, "The oldest oil accumulation in China: Meso-proterozoic Xiamaling Formation bituminous sandstone reservoirs," *Petroleum Exploration and Development*, vol. 38, no. 4, pp. 503–512, 2011.

[44] F. Westall, L. Boni, and E. Guerzoni, "The experimental silicification of microorganisms," *Palaeontology*, vol. 38, pp. 495–528, 1995.

[45] Q.-R. Meng, H.-H. Wei, Y.-Q. Qu, and S.-X. Ma, "Stratigraphic and sedimentary records of the rift to drift evolution of the northern North China craton at the Paleo- to Mesoproterozoic transition," *Gondwana Research*, vol. 20, no. 1, pp. 205–218, 2011.

[46] J. W. Costerton, Z. Lewandowski, D. E. Caldwell, D. R. Korber, and H. M. Lappin-Scott, "Microbial biofilms," *Annual Review of Microbiology*, vol. 49, pp. 711–745, 1995.

[47] A. P. Petroff, N. J. Beukes, D. H. Rothman, and T. Bosak, "Biofilm growth and fossil form," *Physical Review X*, vol. 3, no. 4, Article ID 041012, 2014.

[48] D. G. Davies, M. R. Parsek, J. P. Pearson, B. H. Iglewski, J. W. Costerton, and E. P. Greenberg, "The involvement of cell-to-cell signals in the development of a bacterial biofilm," *Science*, vol. 280, no. 5361, pp. 295–298, 1998.

[49] M. Fletcher, "How do bacteria attach to solid surfaces?" *Microbiological Sciences*, vol. 4, no. 5, pp. 133–136, 1987.

[50] W. Hamilton, *Biofilms: Microbial Interactions and Metabolic Activities*, 1987, Biofilms, Microbial interactions and metabolic activities.

[51] M. Antonio and D. Schulze-Makuch, "Toward a new understanding of multicellularity," *Hypotheses in the Life Sciences*, vol. 2, pp. 4–14, 2012.

[52] H. Ohtsuki, C. Hauert, E. Lieberman, and M. A. Nowak, "A simple rule for the evolution of cooperation on graphs and social networks," *Nature*, vol. 441, no. 7092, pp. 502–505, 2006.

[53] G. G. Anderson and G. A. O'Toole, "Innate and induced resistance mechanisms of bacterial biofilms," *Current Topics in Microbiology and Immunology*, vol. 322, pp. 85–105, 2008.

[54] J. W. Costerton, K. J. Cheng, G. G. Geesey et al., "Bacterial biofilms in nature and disease," *Annual Review of Microbiology*, vol. 41, pp. 435–464, 1987.

[55] V. Venturi, Á. Kerényi, B. Reiz, D. Bihary, and S. Pongor, "Locality versus globality in bacterial signalling: can local communication stabilize bacterial communities?" *Biology Direct*, vol. 5, article no. 30, 2010.

[56] A. Bird, "Themajor transitions in evolution," *Trends in Ecology & Evolution*, vol. 10, no. 9, p. 385, 1995.

[57] C. Pfeffer, S. Larsen, J. Song et al., "Filamentous bacteria transport electrons over centimetre distances," *Nature*, vol. 491, no. 7423, pp. 218–221, 2012.

[58] K. C. Rice and K. W. Bayles, "Death's toolbox: Examining the molecular components of bacterial programmed cell death," *Molecular Microbiology*, vol. 50, no. 3, pp. 729–738, 2003.